

Interfacial Sensing and Evaluation of Carbon and SiC Fibers/ Epoxy Composites with Different Embedding Angle using Electro-Micromechanical Technique

Sang-Il Lee^{**}, Jin-Woo Kong^{*}, Joung-Man Park^{*†}

Electro-Micromechanical Technique 을 이용한 각의 변화에 따른 Carbon 과 SiC Fiber/Epoxy Composites 의 계면감지능 및 평가

이상일^{**} · 공진우^{*} · 박종만^{*†}

KEY WORDS: interfacial sensing, electrical resistivity, embedded angle, Electro-micromechanical technique, nondestructive evaluation(NDE), interfacial shear strength (IFSS)

ABSTRACT

Interfacial properties and electrical sensing for fiber fracture in carbon and SiC fibers/epoxy composites were investigated by the electrical resistance measurement and fragmentation test. As fiber-embedded angle increased, interfacial shear strength (IFSS) of two-type fiber composites decreased, and the elapsed time was long to the infinity in electrical resistivity. The initial slope of electrical resistivity increased rapidly to the infinity at higher angle, whereas electrical resistivity increased gradually at small angle. Furthermore, both fiber composites with small embedded angle showed a fully-developed stress whitening pattern, whereas both composites with higher embedded angle exhibited a less developed stress whitening pattern. As embedded angle decreased, the gap between the fragments increased and the debonded length was wider for both fiber composites. Electro-micromechanical technique can be a feasible nondestructive evaluation to measure interfacial sensing properties depending on the fiber-embedded angle in conductive fiber reinforced composites.

Nomenclature

Ω	: Electrical resistance
ρ	: Measured electrical resistivity
L_{ec}	: Length of fiber contacting to copper wire
d	: Fiber diameter
σ_f	: The single fiber tensile strength
τ	: Interfacial shear strength (IFSS)
α	: Scale parameters in Weibull distribution
β	: Shape parameters in Weibull distribution
Γ	: Gamma function
l_c	: Critical length

1. INTRODUCTION

Using the electrical resistivity measurement, a new evaluation technique of interfacial properties as well as curing characteristics and the residual stress were investigated recently in various conductive fiber reinforced composites. [1-2] The electro-micromechanical technique had been studied as economically a new nondestructive evaluation (NDE) method for monitoring of curing characteristics, interfacial properties and nondestructive behavior because conductive fiber can act as a sensor in itself as well as a reinforcing fiber. [3, 4] Yuse used the electrical resistance measurement as one of the intelligent nondestructive testing (NDT) method. The relationship between electrical resistance and fiber breakage/delamination in carbon fiber reinforced plastic (CFRP) laminate was studied under tensile and fatigue tests.

AE is well known as one of the important NDT methods. The AE can monitor the fracture behavior of composite materials, and can characterize many AE parameters to understand the type of microfailure sources during the fracture progressing. When tensile loading is applied to a composite, AE signal may occur from fiber

^{*}Department of Polymer Science and Engineering,
Research Center for Aircraft Parts Technology,
Gyeongsang National University

^{**}University of Nebraska-Lincoln, U. S. A.

[†]To whom correspondence should be addressed.

fracture, matrix cracking, and debonding at the fiber-matrix interface. AE energy released by the fiber fracture could be greater than that associated by debonding or matrix cracking [5]. Park [6] was studied on micro-mechanical properties and microfailure mechanism of single-carbon fiber composites using AE and fragmentation test.

In this work, or under tensile test, the measurement of electrical resistance and the analysis of AE signals in fiber/epoxy composite were used to evaluate interfacial properties and nondestructive behaviors depending on the different fiber-embedded angle of fiber. The relationship among the electrical resistivity, residual stress, AE signal and IFSS were investigated for single fiber/epoxy composites.

2. EXPERIMENTAL

2.1. Materials

Carbon fiber of 8 μm (Taekwang Industrial Co., Korea) in average diameter and SiC fiber (Ube Industrial Co., Japan) of 13 μm were used as conductive reinforcing materials. Epoxy resin (Kukdo Chemical Co. YD-128, Korea) is based on diglycidyl ether of bisphenol-A (DGEBA). Polyoxypropylene diamene (Jef-famine D400 and D2000, Huntsman Pertochemical Co.) was used as curing agents. The flexibility of specimens was controlled by the mixing ratio of D-400 versus D-2000.

2.2. Methodologies

2.2.1. Preparation of Testing Specimens

The type specimens were used for fragmentation test, curing monitoring and electro-micromechanical test. Figure 1(a) exhibits a testing specimen to evaluate electrical resistivity as a function of various embedded angles by the electro-micromechanical testing. Figure 1(b) shows dogbone-type specimen that is single carbon fiber composites to measure IFSS and AE signals.

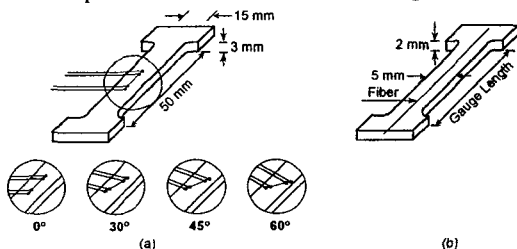


Fig. 1. Test specimen of single fiber composites for (a) electrical resistivity and (b) IFSS and AE signal

2.2.2. Electrical Resistance Measurements

The electrical resistance was measured using a HP34401A digital multimeter. For the electrical resistance measurement under tensile load, the stress-strain curve was measured by universal testing machine

(UTM, Loyd Instruments Co., U.K.). Electrical resistivity was obtained from the measured electrical resistance, cross-sectional area of the conductive fiber, A , and electrical contact length, L_{ec} of the testing fiber connecting to copper wire. The relationship between electrical resistivity, ρ and resistance, R is as follow:

$$\rho (\Omega \cdot \text{cm}) = \frac{A}{L_{ec}} \times R \quad (1)$$

Figure 2(a) is experimental schemes showing the measurement of electrical resistance and stress-strain curve in single fiber composite.

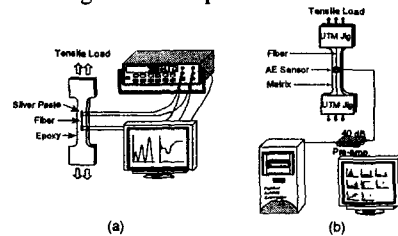


Fig. 2. Experimental system for (a) electrical resistivity measurement and (b) acoustic emission

2.2.3. IFSS Measurement and AE Test

To evaluate IFSS and AE signals depending on the embedded angle, UTM was used with a polarized-light microscope and AE system. The specimens were tested by UTM (load cell of 10kN, speed rate of 0.5 mm/second) while AE monitoring. After the testing specimen was fixed in the tensile testing machine, the composite was strained incrementally and the fiber was broken into small fragments embedded in the matrix until no longer fiber fracture occurred.

IFSS was determined by Drzal equation [7] that was modified from Kelly-Tyson equation [8]. By introducing the Weibull distribution for the aspect ratio, IFSS was exhibited in the form as follows:

$$\tau = \frac{\sigma_f}{2 \cdot \alpha} \cdot \Gamma [1 - 1/\beta] \quad (3)$$

Where α and β are scale and shape parameters of Weibull distribution for aspect ratio (l_c/d), and Γ is the gamma function.

AE signals were detected using a miniature sensor (Resonance Type, PICO by PAC) with peak sensitivity of 54 Ref V(m/s) and resonant frequency at 500 kHz. The sensor output was amplified by 40 dB at preamplifier gain. The threshold level was set up as 30 dB. The signal was fed into an AE signal process unit (MISTRAS 2001), where AE parameters were analyzed using in-built software. The typical AE parameters such as hit rate, peak amplitude, and event duration were investigated for the time and the distribution analysis. Figure 2(b) shows schematic AE diagram.

3. RESULTS AND DISCUSSION

3.1. Electrical Properties of Two Conductive Fibers

Table 1 Wave velocity of epoxy matrix as curing agent content

Fiber	Diameter (μm)	Electrical Resistance (Ω)	Electrical Resistivity ($\Omega\cdot\text{cm}$) $\times 10^{-3}$
Carbon ¹⁾	8	1.19×10^4 (570) ⁵⁾	1.86 (0.09)
Carbon ²⁾	18	1.57×10^3 (120)	1.25 (0.10)
SiC ³⁾	10	8.79×10^5 (0.3×10^5)	215.7 (7.4)
SiC ⁴⁾	13	8.36×10^6 (0.1×10^5)	346.6 (6.7)

1) PAN-based (Taekwang Industrial Co., Korea)
 2) Coal-Tar Pitch-based (Mitsubishi Chemical Co., Japan)
 3), 4) Silicon Carbide-based fiber (Ube Industrial Co., Japan)
 5) Parenthesis is standard deviation.

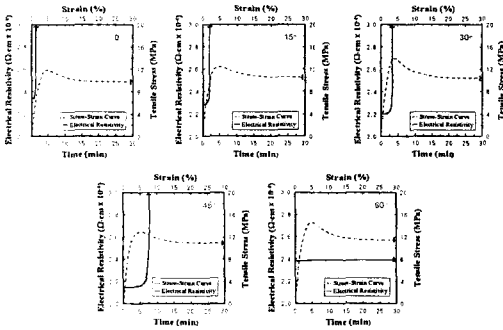


Fig. 3 Electrical resistivity and stress-strain curve in carbon fiber composites

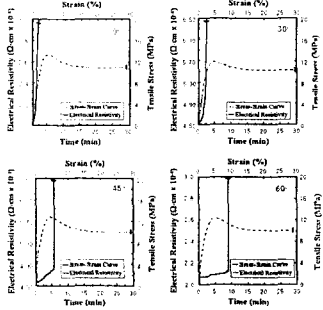


Fig. 4 Electrical resistivity and stress-strain curve in carbon fiber composites

Table 1 shows intrinsically electrical properties of two conductive fibers. Electrical resistance was measured by four-points probe method. Silver paste was used as electrically connecting glue at junctions to maintain an electrical contact between the fiber and leading wire.

Figure 3 and 4 show electrical resistivity and stress-strain curve in single carbon and SiC fiber/epoxy composites. As the fiber-embedded angle increased, elapsed time to the infinity in electrical resistivity increased and initial slope of electrical resistivity also gradually increased.

3.2. Interfacial Properties of Single Fiber/Epoxy Composites

Table 2 shows interfacial properties and statistical Weibull parameters of single carbon and SiC fiber/

epoxy composites with fiber-embedded angles. As the fiber embedded angle increased, the average fragment length and aspect ratio, l/d , were larger and IFSS decreased.

Table 2 Interfacial properties of carbon and SiC fiber composites

Embedding Angle (Degree)	Carbon Fiber Composites					SiC Fiber Composites		
	Critical Fragment Length (μm)	Aspect Ratio (l/d)	Scale Parameter (α)	Shape Parameter (β)	IFSS (MPa) Kelly ¹⁾ Drzal ²⁾	Critical Fragment Length (μm)	Aspect Ratio (l/d)	IFSS ³⁾ (MPa)
0	533.5	66.7	72.2	5.43	37.1 35.0	871	67	35.1
15	614.3	76.8	83.1	5.50	31.3 29.6	-	-	-
30	757.1	94.6	102.2	5.61	24.4 23.2	1162	89	25.5
45	888.9	111.11	120.5	5.20	20.4 19.1	1477	114	19.3
60	-	-	-	-	-	1747	134	16.0

1) Calculated from Kelly-Tyson equation
 2) Calculated from Drzal equation
 3) Calculated from Kelly-Tyson equation
 * 5 specimens were used to evaluate IFSS

Figure 5 shows IFSS and aspect ratio depending on fiber-embedded angles. In case of single carbon fiber/epoxy composite, IFSS of 60 degree was not measured, because the fiber of 60 degree was not broken.

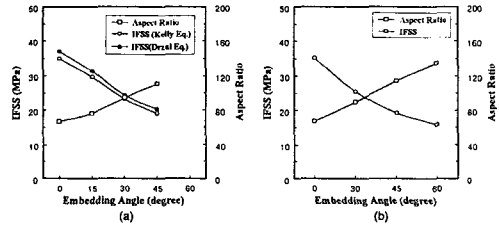


Fig. 5 IFSS and aspect ratio depending on embedded fiber angle

3.3. Microfailure Modes

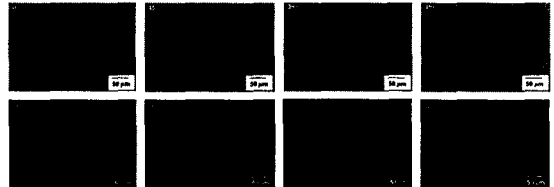


Fig. 6 Initial fiber failure modes and stress whitening of carbon fiber composites

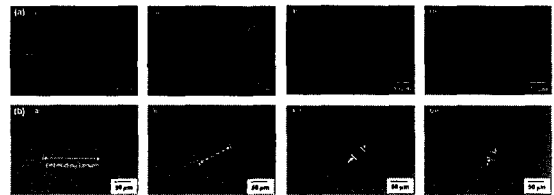


Fig. 7 (a) Initial stress whitening and (b) final debonding length of SiC fiber composites

Figure 6 shows the comparison of fully developed whitening and initial fiber failure modes of carbon fiber/epoxy composites. As the fiber-embedded angle increased fully developed stress birefringence pattern

was smaller. Strains of first fiber breakage are 1.18 % of 0 degree, 2.7 % of 15 degree, 4.0 % of 30 degree and 7.8% of 45 degree, respectively. The fiber of 60 degree was not break. The first fiber breakage occurred late as the fiber-embedded angle increased. As shown figure 6 and 7, when the fiber was broken, the crack shape of matrix was not cone shape. Because the transferring load to matrix was very small, the matrix crack was not shown.

Figure 7 is initial and/or final microfailure modes of SiC fiber/epoxy composites. As the fiber-embedded angle decreased, birefringence pattern of fully developed stress was same with carbon fiber case and the gap between fragments increased.

3. 4. AE Results

Figure 8 and 9 show result of AE energy and AE amplitude and Figure 10 shows AE waveforms of single carbon fiber composites. AE energy and AE amplitude of small angle were higher than high case and the main signal group appeared late in the elapsed time.

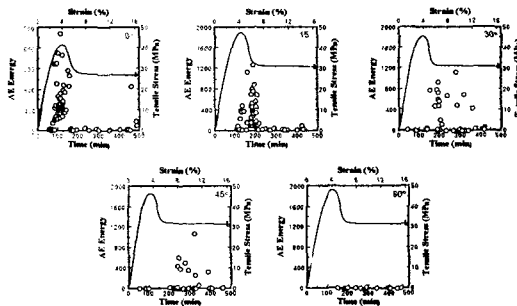


Fig. 8 AE energy and Stress-strain curve depending on embedded fiber angle

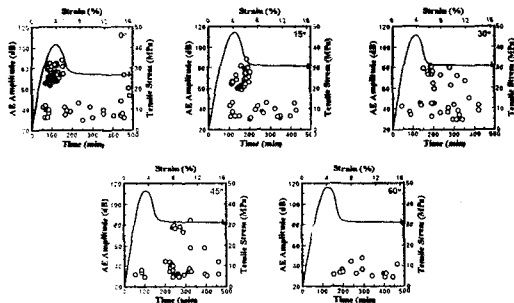


Fig. 9 AE amplitude and Stress-strain curve depending on embedded fiber angle

As the fiber-embedded angle increased, fiber signals reduced and the voltage of AE waveform decreased smaller. This might be due to the difference in microfailure mechanisms depending on fiber-embedded angles. In carbon fiber composite, fiber fracture was not occurred in 60 degree.

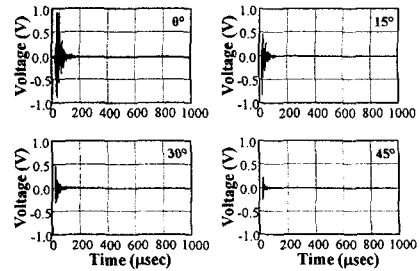


Fig. 10 Electrical resistivity and stress-strain curve in carbon fiber composites

4. CONCLUSIONS

Electrical resistance of carbon and SiC fiber composites was responded well during the measurement of interfacial sensing properties. As the fiber-embedded angle increased, the elapsed time to the infinity for electrical resistivity increased. As fiber-embedded angle decreased, IFSS increased and the elapsed time was faster to infinity at the first fiber fracture in both two fibers. The specimen with small angle showed a fully developed stress whitening pattern, whereas that with higher angle showed a less developed stress whitening pattern. AE events were detected well under tensile load. As the fiber-embedded angle increased, AE energy was gradually smaller and main signal groups appeared late in the elapsed time. AE voltage of the waveform of carbon fiber breaks in the small angle exhibited much larger than that in higher angle.

ACKNOWLEDGMENT: This work was financially supported by Research Center for Aircraft Parts Technology (ReCAPT), GNU.

REFERENCES

- (1) D. M. Bontea, D.D. Chung, and G. C. Lee, *Cem. & Conc. Res.*, 30, 2000, p. 651.
- (2) K. Yuse and C. Bathias, *In Proceeding ICCM-12. Paris. France, 1999*, p. 767.
- (3) X. Wang and D. D. L. Chung, *Compos. Interf.*, 5, 1998, p. 277.
- (4) X. Wang and D. D. L. Chung, *Compos. Interf.*, 5, 1998, p. 191.
- (5) J. M., Park, W. G. Shin and D. J. Yoon, *Compos. Sci. Tech.*, 59, 1999, p. 355.
- (6) J. M., Park, E. M. Chong, D. J. Yoon and J. H. Lee, *Polym. Compos.*, 11, 1998, p. 747.
- (7) L. T. Drzal, *Mater. Sci. Eng.*, 21, 1990, p. 289.
- (8) A. Kelly and W. R. Tyson, *Mech. and Phys. Solids*, 13, 1965, p. 329.